

## Supplementary Material

### **Novel 2-benzoyl-6-(2,3-dimethoxybenzylidene)-cyclohexenol confers selectivity towards human *MLH1* defective cancer cells through synthetic lethality**

Dedrick Soon Seng Song<sup>1</sup>, Sze Wei Leong<sup>2</sup>, Kwok Wen Ng<sup>1,3</sup>, Faridah Abas<sup>2,4</sup>, Khozirah Shaari<sup>2,5</sup>, Chee Onn Leong<sup>6</sup>, Felicia Fei-Lei Chung<sup>6,7</sup>, Chun Wai Mai<sup>6,8</sup>, Ling Wei Hii<sup>6</sup>, Pei Jean Tan<sup>1\*</sup>, Vyomesh Patel<sup>1</sup>

<sup>1</sup>Cancer Research Malaysia, 1 Jalan SS12/1A, Subang Jaya, 47500 Selangor, Malaysia.

<sup>2</sup>Laboratory of Natural Products, Institute of Bioscience, Universiti Putra Malaysia, 43400 UPM Serdang, Selangor, Malaysia.

<sup>3</sup>Centre of Foundation Studies, Universiti Teknologi MARA, Persiaran Cybersouth, 43800, Selangor, Malaysia.

<sup>4</sup>Department of Food Science, Faculty of Food Science and Technology, Universiti Putra Malaysia, 43400 UPM Serdang, Selangor, Malaysia.

<sup>5</sup>Department of Chemistry, Faculty of Science, Universiti Putra Malaysia, 43400 UPM Serdang, Selangor, Malaysia.

<sup>6</sup>Center for Cancer and Stem Cell Research, International Medical University, Bukit Jalil, Malaysia

<sup>7</sup>Mechanisms of Carcinogenesis (MCA), Epigenetics Group (EGE), International Agency for Research on Cancer World Health Organization, Lyon, CEDEX 08, France

<sup>8</sup>School of Pharmacy, International Medical University, Bukit Jalil, Malaysia

\*Correspondence

Pei Jean Tan

Email: peijean.tan@cancerresearch.my

F: 603-2712 3225

T: 603-2712 3224

**Keywords:** Mismatch repair, MLH1, synthetic lethality, diarylpentanoid, cancer

## Supplementary Figures

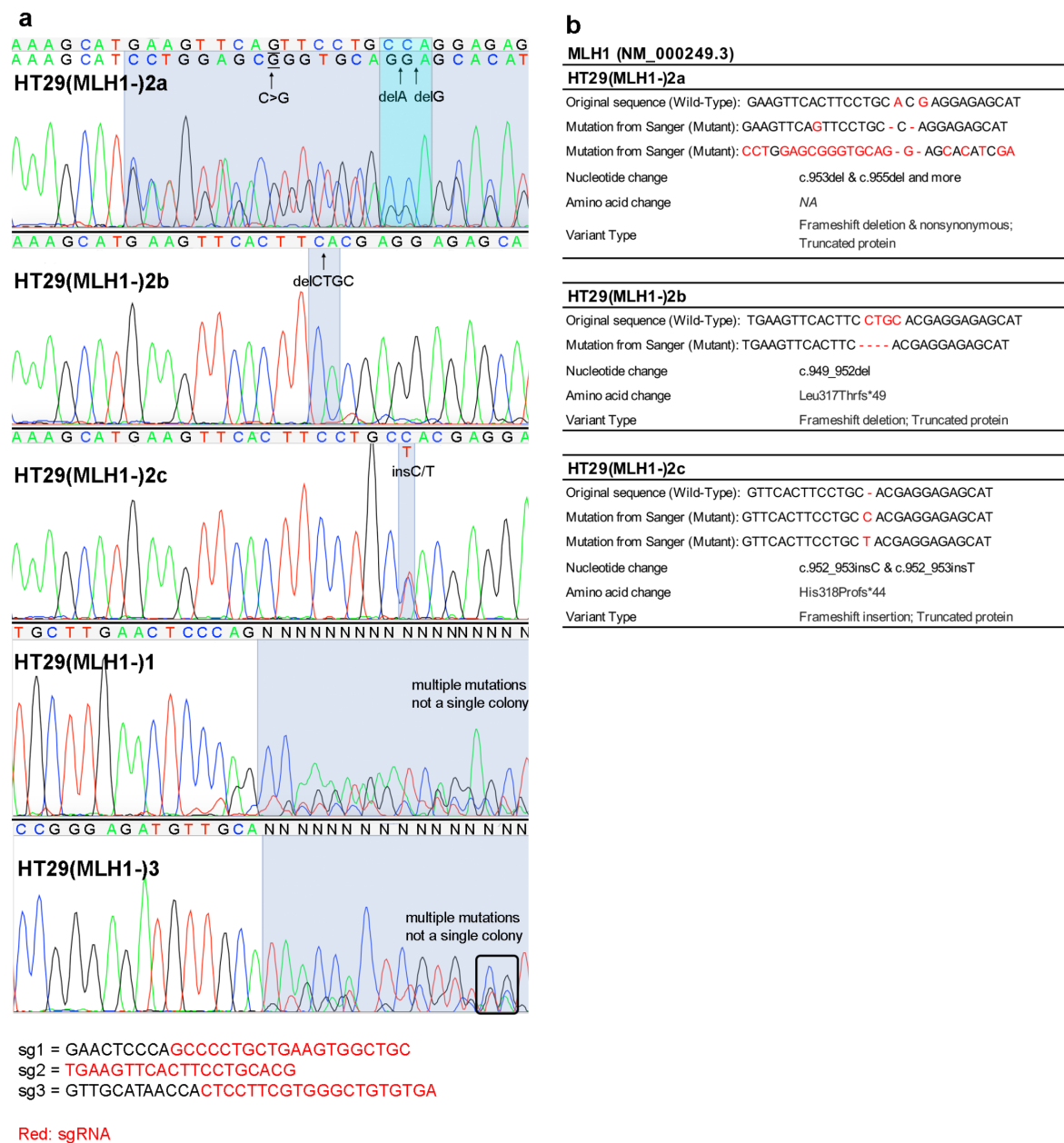


**Fig. S1 MLH1 mutational status in HT29 (-/-) knock-outs.** HT29 treated with lentiviral particles containing sgRNA sequences sg1, sg2 and sg3. Single colonies for each sgRNA treatment were selected and grown; HT29(MLH1-)-1 derived from sg1; HT29(MLH1-)-2a, HT29(MLH1-)-2b and HT29(MLH1-)-2c derived from sg2; HT29(MLH1-)-3 derived from sg3. The mutational profiles of each have been mapped out, however HT29(MLH1-)-1 and HT29(MLH1-)-3 have multiple mutations likely indicating that presence of multiple colonies. (a) Chromatograph of MLH1 mutational status in HT29(MLH1-)-1, HT29(MLH1-)-2a,

HT29(MLH1-)-2b, HT29(MLH1-)-2c and HT29(MLH1-)-3. **(b)** Summary of mutational profiles of HT29(MLH1-)-2a, HT29(MLH1-)-2b and HT29(MLH1-)-2c.

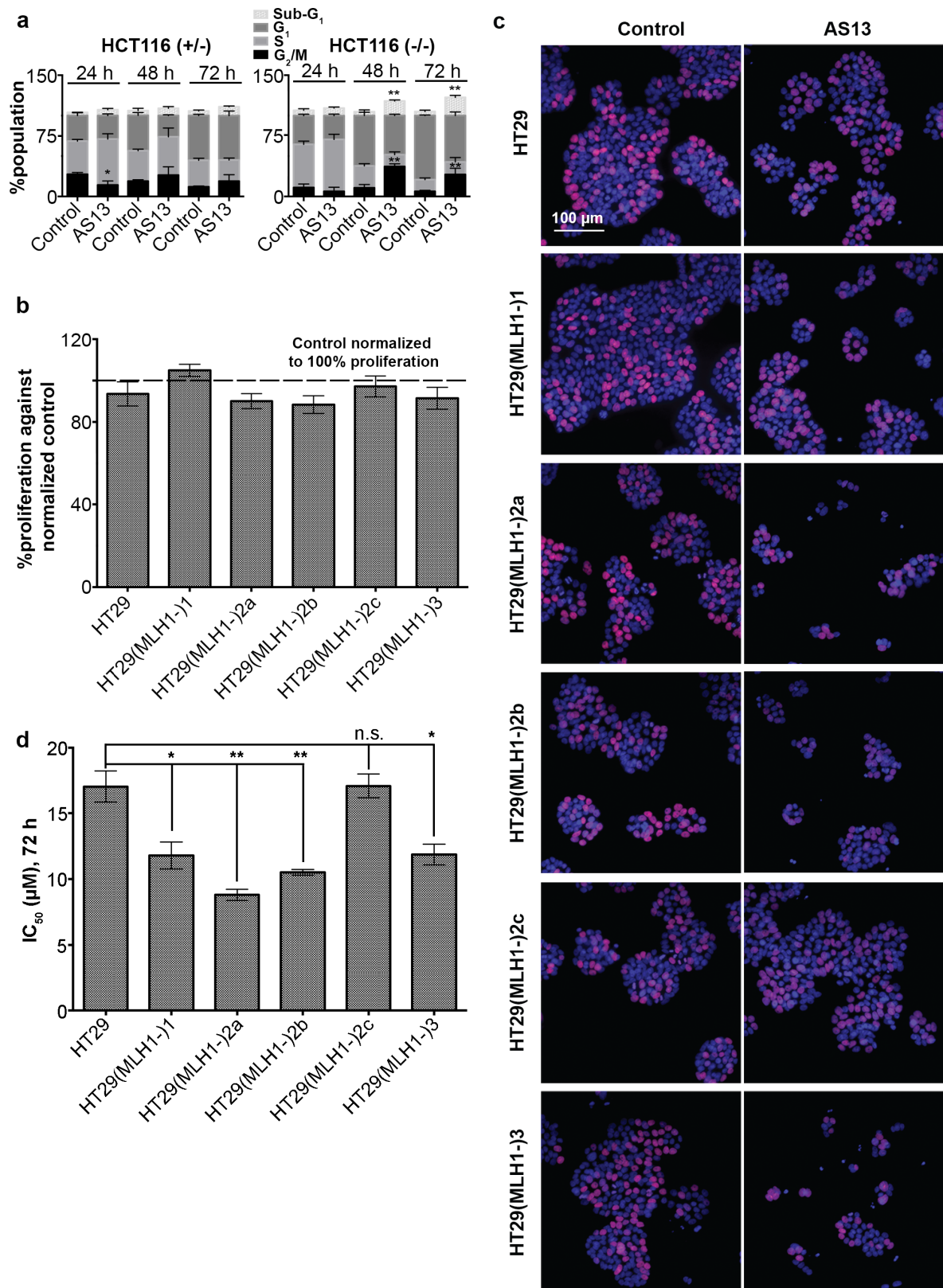


**Fig. S2 Non-significant changes in cell cycle and proliferation of HT29 MLH1 knock-outs compared to HT29 and the effect of menadione treatment. (a)** Cell cycle data of G<sub>1</sub>, S,

G<sub>2</sub>/M populations of HCT116 isogenics with AS13 (10 μM) and control for 24, 48 and 72 h. Sub-G<sub>1</sub> population was determined by the number of cell population at sub-G<sub>1</sub> over total cell population. \* depicted statistically significant compare to the controls with  $p < 0.05$ ; \*\* depicted  $p < 0.01$ . **(b)** Cell proliferation of HT29 and *MLH1* knock-outs (HT29(MLH1-)-1, HT29(MLH1-)-2a, HT29(MLH1-)-2b, HT29(MLH1-)-2c and HT29(MLH1-)-3) upon AS13 (50 μM, 72 h) was measured by the amount of incorporated EdU over viable cells by immunofluorescence (an average of seven representative fields). Data has been normalised to its control cell line, whereby 100% represents the control proliferation. **(c)** Representative merge images from **(b)**. Blue represents nuclei stained viable cells while pink represents the EdU-Alexa 568 incorporated proliferation cells. Scale 100 μm **(d)** Half maximal inhibitory concentrations (IC<sub>50</sub>) of menadione (72 h) were measured using MTT cell viability assay. \* depicted statistically significant compare to the HT29 *MLH1* proficient cells  $p < 0.05$ ; \*\* depicted  $p < 0.01$ .

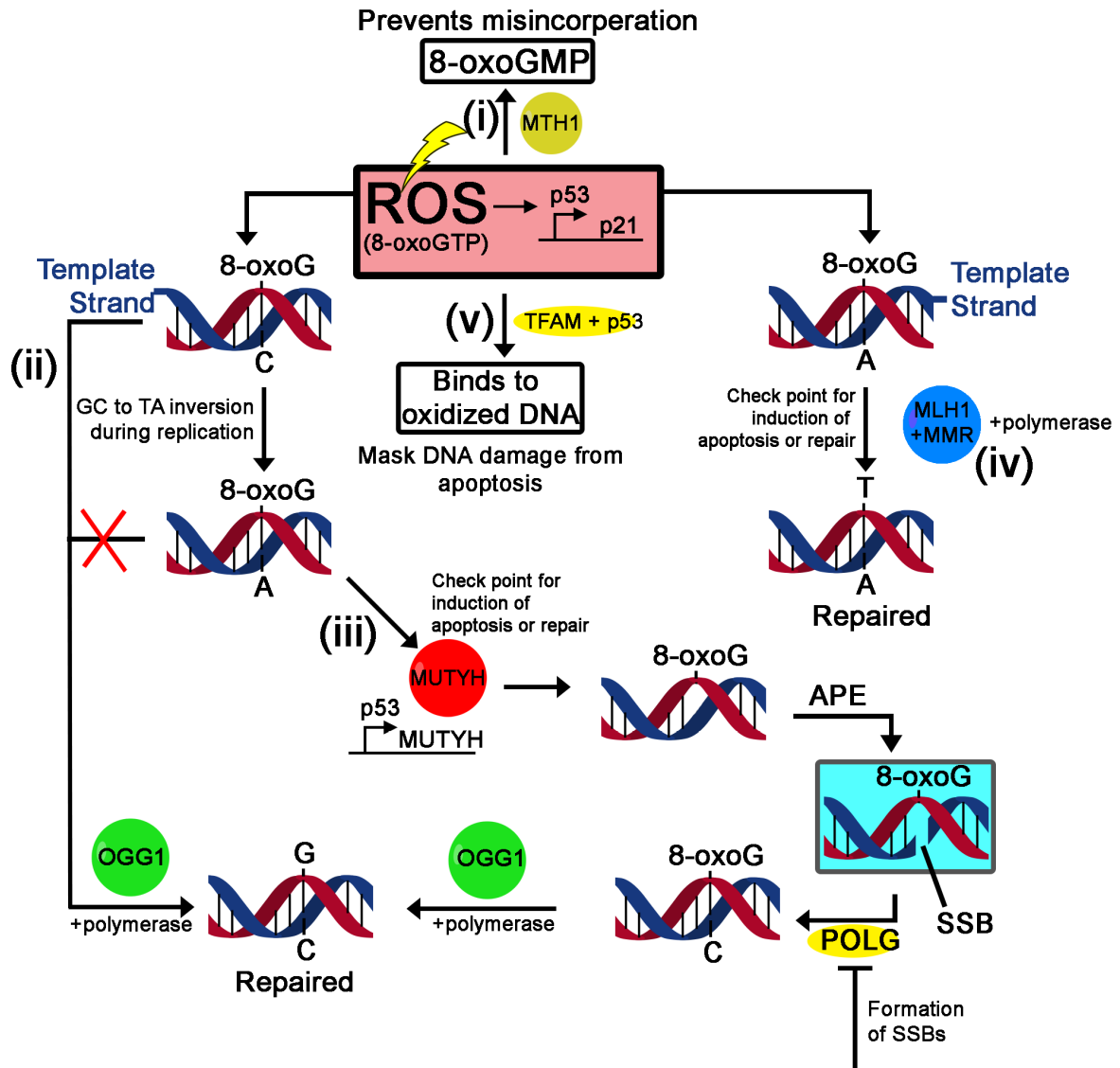


**Fig. S3 DNA repair pathways for 8-oxoG lesions in the mitochondria.** 8-oxoG when left unrepaired will cause the conversion of GC to TA mutations. In mtDNA, there are thought to be five major DNA repair pathways that are responsible for the prevention of these oxidised lesions. (i) MutT homolog-1 (MTH1) hydrolyses 8-oxoGTP into the monophosphate form hence preventing mis-incorporation/transversion of base pairs during DNA replication.<sup>1,2</sup> (ii) 8-oxoG:C pairs are thought to be mainly detected by OGG1 and performs the first step of base excision repair (BER) by removing the 8-oxoG paired with cytosine.<sup>3</sup> (iii) 8-oxoG:A mismatch pairs are recognised by MUTYH and with APE endonuclease, excises mis-incorporated adenine in the nascent DNA strand. This allows POLG to correctly insert cytosine opposite 8-

oxoG creating a substrate for OGG1.<sup>4</sup> MUTYH is known to be regulated by p53.<sup>5</sup> Inhibition of POLG will lead to unrepaired 8-oxoG:SSBs ultimately leading to formation of lethal DSBs.<sup>6</sup> (iv) In 8-oxoG:A where adenine is the template strand, it is been thought that the mismatch repair, MLH1, contribute to the removal of 8-oxoG in the nascent strand.<sup>7, 8</sup> (v) The transcription factor A mitochondrial (TFAM), is known to bind to oxidised DNA under oxidative stress masking the damage and preventing apoptosis.<sup>9</sup>

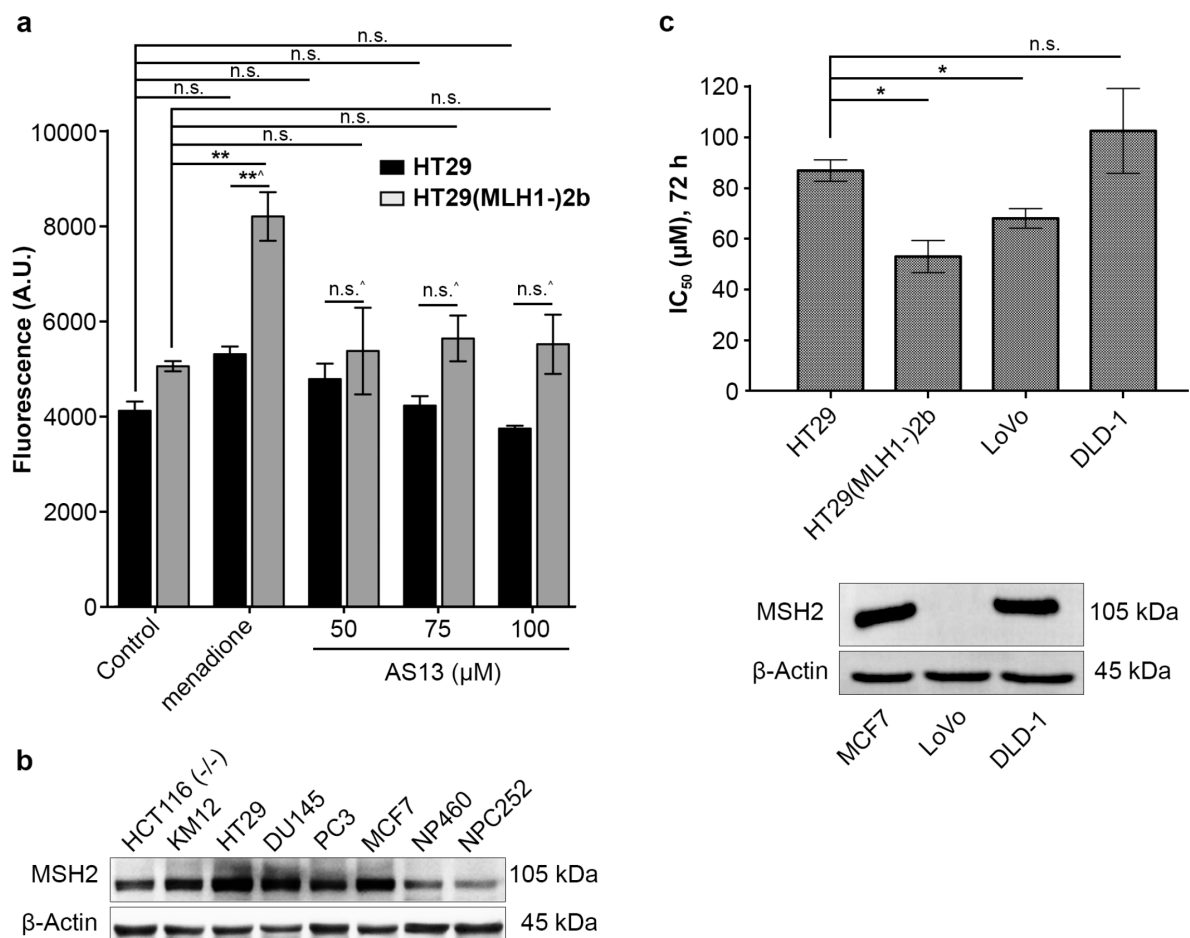
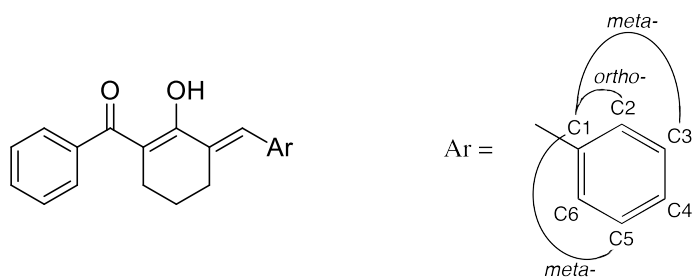


**Fig. S4 Effect of AS13 dose dependent induction of double strand breaks and MSH2/MSH6 deficient lines. (a)** Quantification of double stranded breaks (24 h) in HT29 and HT29(MLH1)-2b with increasing AS13 concentration (50-100 μM) and menadione (12.5 μM) were performed by the analysis of the surrogate marker  $\gamma$ -H2A.X in conjugation with a fluorophore. The fluorescence geometric mean was analysed using flow cytometry. **(b)**

Immunoblot of *MSH2* basal expression on a panel of *MLH1* proficient and deficient cancer cell lines with  $\beta$ -actin as loading control. (c) Half maximal inhibitory concentration ( $IC_{50}$ ) of AS13 (72 h) were measured by MTT cell viability assay and immunoblot of *MSH2* basal expression of MCF7, LoVo and DLD-1.

## Supplementary Tables

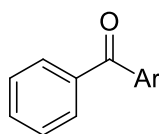


**Supplementary Table S1A.** Half maximal inhibitory concentration ( $IC_{50}$ ) of curcumin, AS1-24 and AS30-31 with aryl substituent modification against HCT116 *MLH1* isogenic pairs at 72 h MTT assay

Compounds	Ar	$IC_{50} \pm SEM$ ( $\mu M$ ), 72 h (n $\geq$ 3)		Fold Change
		HCT116 (+/-)	HCT116 (-/-)	
<b>Curcumin</b>	-	9.76 $\pm$ 2.16	9.38 $\pm$ 2.28	1.04
<b>AS1</b>	Phenyl	N.I	N.I	-
<b>AS2</b>	2-methoxyphenyl	98.1 $\pm$ 7.90	N.I	-
<b>AS3</b>	3-methoxyphenyl	52.7 $\pm$ 2.68	55.5 $\pm$ 4.45	0.95
<b>AS4</b>	4-methoxyphenyl	N.I	N.I	-
<b>AS5</b>	2-chlorophenyl	41.0 $\pm$ 3.98	41.8 $\pm$ 2.12	0.98
<b>AS6</b>	3-chlorophenyl	37.6 $\pm$ 3.67	38.4 $\pm$ 5.39	0.98
<b>AS7</b>	4-chlorophenyl	83.3 $\pm$ 4.29	93.0 $\pm$ 7.00	0.90
<b>AS8</b>	3-hydroxyphenyl	39.2 $\pm$ 5.76	34.5 $\pm$ 4.48	1.14
<b>AS9</b>	4-hydroxyphenyl	54.8 $\pm$ 2.31	55.9 $\pm$ 4.75	0.98
<b>AS10</b>	3,4-dihydroxyphenyl	22.6 $\pm$ 4.45	16.2 $\pm$ 3.36	1.40
<b>AS11</b>	Naphthalen-1-yl	N.I	N.I.	-
<b>AS12</b>	Naphthalen-2-yl	N.I	N.I.	-
<b>AS13</b>	2,3-dimethoxyphenyl	25.8 $\pm$ 3.01	9.53 $\pm$ 1.98	2.71
<b>AS14</b>	2,5-dimethoxyphenyl	34.2 $\pm$ 5.37	35.9 $\pm$ 2.26	0.95
<b>AS15</b>	3,4-dimethoxyphenyl	30.0 $\pm$ 6.68	27.7 $\pm$ 3.64	1.08
<b>AS17</b>	4-hydro-3-methoxyphenyl	46.5 $\pm$ 6.88	48.9 $\pm$ 3.73	0.95
<b>AS18</b>	3-hydroxy-4-methoxyphenyl	33.9 $\pm$ 7.57	28.7 $\pm$ 5.53	1.18
<b>AS19</b>	3-chloro-4-hydroxyphenyl	61.1 $\pm$ 7.11	49.4 $\pm$ 7.52	1.24

AS20	3-bromo-4-hydroxyphenyl	42.1 ± 6.31	38.4 ± 6.01	1.10
AS21	5-methylfuran-2-yl	59.4 ± 6.65	79.5 ± 4.50	0.75
AS23	Thiophen-2-yl	46.3 ± 4.35	54.1 ± 4.17	0.86
AS24	5-methylthiophen-2-yl	77.9 ± 5.32	93.5 ± 6.25	0.83
AS30	3-fluorophenyl	35.5 ± 6.37	45.9 ± 7.03	0.77
AS31	2,3,4-trimethoxyphenyl	38.2 ± 5.94	58.5 ± 5.28	0.65

N.I: No inhibition at the highest test concentration 100  $\mu$ M



**Supplementary Table S1B.** Half maximal inhibitory concentration ( $IC_{50}$ ) of AS25-29 and AS32 with xanthene moiety modification against HCT116 *MLH1* isogenic pairs at 72 h using MTT viability assay

Compounds	Ar	$IC_{50} \pm SEM$ ( $\mu$ M)		Fold change
		HCT116 (+/-)	HCT116 (-/-)	
AS26	4-benzoyl-5-hydroxy-1,2,3-trihydroxanthene	61.0 ± 5.27	63.1 ± 7.13	0.97
AS27	4-benzoyl-6-hydroxy-1,2,3-trihydroxanthene	N.I	N.I	-
AS28	4-benzoyl-7-hydroxy-1,2,3-trihydroxanthene	36.1 ± 6.14	47.6 ± 5.64	0.76
AS29	4-benzoyl-6,8-dimethoxy-1,2,3-trihydroxanthene	20.9 ± 6.09	14.2 ± 4.77	1.47
AS32	4-benzoyl-1,2,3-trihydroxanthene	51.9 ± 4.93	53.3 ± 7.30	0.97

N.I: No inhibition at the highest test concentration 100  $\mu$ M

## Supplementary References

1. Yoshimura D.; Sakumi K.; Ohno M. et al. An oxidized purine nucleoside triphosphatase, mth1, suppresses cell death caused by oxidative stress. *J Biol Chem.* **2003**, *278*, 37965-73.
2. Abdel-Rahman W. M.; Ruosaari S.; Knuutila S. et al. Differential roles of eps8 in carcinogenesis: Loss of protein expression in a subset of colorectal carcinoma and adenoma. *World J Gastroenterol.* **2012**, *18*, 3896-903.
3. Nishioka K.; Ohtsubo T.; Oda H. et al. Expression and differential intracellular localization of two major forms of human 8-oxoguanine DNA glycosylase encoded by alternatively spliced ogg1 mRNAs. *Mol Biol Cell.* **1999**, *10*, 1637-52.
4. Ichinoe A.; Behmanesh M.; Tominaga Y. et al. Identification and characterization of two forms of mouse mutyh proteins encoded by alternatively spliced transcripts. *Nucleic Acids Res.* **2004**, *32*, 477-87.
5. Oka S.; Leon J.; Tsuchimoto D. et al. Mutyh, an adenine DNA glycosylase, mediates p53 tumor suppression via parp-dependent cell death. *Oncogenesis.* **2014**, *3*, e121.
6. Martin S. A.; McCabe N.; Mullarkey M. et al. DNA polymerases as potential therapeutic targets for cancers deficient in the DNA mismatch repair proteins msh2 or mlh1. *Cancer Cell.* **2010**, *17*, 235-48.
7. Gu Y.; Parker A.; Wilson T. M. et al. Human muty homolog, a DNA glycosylase involved in base excision repair, physically and functionally interacts with mismatch repair proteins human muts homolog 2/human muts homolog 6. *J Biol Chem.* **2002**, *277*, 11135-42.
8. Repmann S.; Olivera-Harris M.; Jiricny J. Influence of oxidized purine processing on strand directionality of mismatch repair. *J Biol Chem.* **2015**, *290*, 9986-99.
9. Yoshida Y.; Izumi H.; Torigoe T. et al. P53 physically interacts with mitochondrial transcription factor a and differentially regulates binding to damaged DNA. *Cancer Res.* **2003**, *63*, 3729-34.

